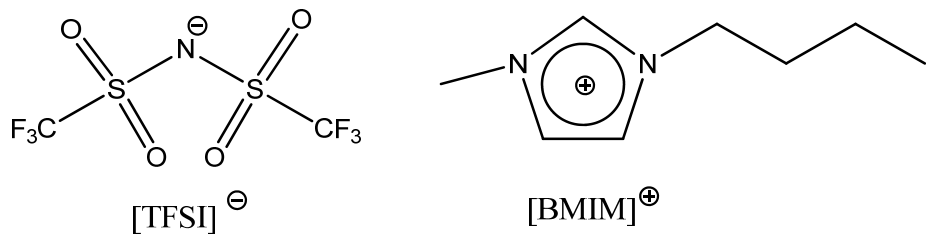


Electronic Supplementary Information

"Autocatalytic Sonolysis of Iron Pentacarbonyl in Room Temperature Ionic Liquid

[BuMeIm][Tf₂N]"



Scheme 1S. Shematic representation of [BuMeIm][Tf₂N].



Figure 1S. Cup-horn sonochemical reactor without direct contact of sonicated liquid with ultrasonic emitter.

0,7 mL of $\text{Fe}(\text{CO})_5$ (5.25 mmol) and 10 ml of dried (<100 ppm H_2O) ionic liquid $[\text{BuMeIm}][\text{Tf}_2\text{N}]$ were placed in a round bottom Schlenck tube made from Pyrex glass of 1 mm wall thickness and purged with argon in an argon filled glove box (0.1 ppm O_2). The tube was then placed in a cap horn ultrasonic cell equipped with Vibra cellTM 75041 generator operating at the ultrasonic frequency of 20 kHz. Steady-state temperature inside the reaction vessel equal to 5°C was provided by circulation of cooled silicon oil through cap-horn cell. The temperature was maintained using a Huber Unistat Tango thermo-cryostat. Silicon oil also provided the transmission of ultrasonic vibrations from emitter to the reaction vessel. The cap-horn reactor allowed to use a small volume of RTIL without direct contact with titanium sonotrode. The experiments in tetralin solutions were performed at the same experimental conditions. The specific absorbed acoustic power P_{ac} ($\text{W}\cdot\text{mL}^{-1}$), transmitted to the RTIL solution was measured by chemical method based on the measurements of hydrogen peroxide formation during pure water sonolysis in argon as described in the literature (See S. I.

Nikitenko et al. *Ultrasonics Sonochemistry* **2007**, 14, 330). The value of P_{ac} in the experiments was found to be equal $0.53 \text{ W}\cdot\text{mL}^{-1}$. The kinetics of CO emission during sonolysis was followed using PROLAB 300 gaseous mass spectrometer (Thermo Fisher) at $E = -40 \text{ eV}$ with Channeltron multiplier detector. The outlet gas was sampled and analyzed each 10 seconds. After sonication the tightly closed tube with reaction mixture was transferred into the glove-box, solid product was removed from RTIL with 0.4T permanent magnet, washed twice with anhydrous THF and dried under vacuum. Low-resolution TEM measurements were carried out at 100kV with a microscope JEOL 1200 EXII. The particles size distribution histograms were determined using enlarged TEM micrographs taken at magnification of $\times 50K$. A large number of nanoparticles (400-600) were counted in order to obtain a size distribution with good statistics. Powder XRD patterns were recorded at room temperature on a Bruker AXS D8 ADVANCE diffractometer with Vario1 Johansson focusing monochromator using Cu K α radiation (0.1540598 nm) and a fixed power source (40 kV , 40 mA). FTIR spectra were recorded with a Perkin Elmer 1600 spectrometer with a 4 cm^{-1} resolution spectrometer using ATR crystal. Magnetic susceptibility data were collected with a Quantum Design MPMS-XL SQUID magnetometer working in the temperature range of $100 - 350 \text{ K}$ and the magnetic field range of $0 - 50 \text{ kOe}$. In the ZFC experiment, the sample was cooled in the absence of a static magnetic field and the magnetization was then recorded as a function of the temperature under a 1000 Oe field. Similarly, the FC magnetization data were collected after cooling the sample with the 1000 Oe probe field applied. All of the chemical reagents used in these experiments were analytical grade. [BuMeIm][Tf₂N] was synthesized according to previously published procedure.^[5] The quantity of water was controlled by Karl-Fisher method and maintained at less than 0.2 wt %.

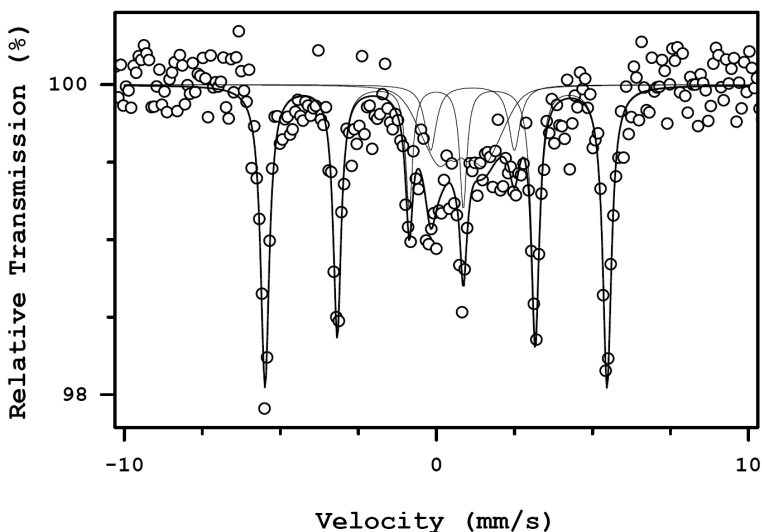


Figure 2S. ^{57}Fe Mössbauer spectrum at 77 K of the Fe nanoparticles into BuMeIm [Tf₂N].

Mössbauer spectra:

^{57}Fe Mössbauer spectra were measured with a source of ^{57}Co in rhodium metal. The measurements were performed in a liquid nitrogen flow cryostat, with the source at ambient temperature (294 K) and the absorber at 77 K. For all measurements, the spectrometer was operated with a triangular velocity waveform, and a NaI scintillation detector was used for the detection of the gamma rays. The spectra were fitted with appropriate superpositions of Lorentzian lines using the PC-Mos II [G. Grosse, Technische Universität München Munich (Germany), 1993] computer program. In this way spectral parameters such as the isomer shift (δ), the electric quadrupole splitting (Δ), the full linewidth at half maximum (Γ_{exp}), the magnetic hyperfine field (B) and the relative resonance areas (A) of the different components of the absorption patterns were determined. These parameters are reported in Table M2. The isomer shifts are given relative to α -iron at room temperature. In order to prevent oxidation of the iron metal particles, the Mössbauer absorbers were prepared by transferring the Fe NPs into IL from the synthesis vessel to a sealed coffee-bag holder in a glovebox under ultra-pure argon atmosphere.

In the ^{57}Fe Mössbauer spectrum of the measured sample, (Figure 2S), at least three different spectral components can be detected. The most intense component, accounting for more than half of the total measured resonance area, is a narrow magnetic sextet with hyperfine parameters typical of iron metal (cf. Table M2). Even though the temperature dependence of this spectrum has not been measured, one can safely assume that this represents iron metal nanoparticles. It is interesting to notice that the isomer shift for this

species is slightly higher than the expected value by about 0.03 mm/s compared to bulk iron, reflecting a rather large second order Doppler shift for this component. The latter would imply a smaller average Debye temperature compared to bulk metal, in agreement with the presence of iron nanoparticles loosely bound to the surrounding solidified ionic liquid environment. The smaller of the other two spectral components, accounting for less than 10 % of the total resonance area, is a quadrupole doublet with parameters in the range of divalent iron. This component resembles those usually observed for similar samples exposed to air, and thus represents decomposition products formed by the oxidation of a small fraction of the iron precursor. The third component accounts for around 35 % of the total resonance area and has been fitted with a broad single Lorentzian with an isomer shift in between those of divalent and trivalent iron. The broadness of this component and its average isomer-shift allow one to attribute it to an ill-defined magnetite-like phase undergoing superparamagnetic relaxations and beginning to order magnetically. This component might represent a slight contamination of Fe nanoparticles by oxide.

Table 1S. ^{57}Fe Mössbauer parameters for the sample containing iron nanoparticles in ionic liquid at 77 K.

Sample	B [T]	Δ [mm/s]	δ [mm/s]	Γ_{exp} [mm/s]	Area [%]
-	34.0(1)	-0.01(1)	0.10(1)	0.31(2)	54(2)
	-	2.59(6)	1.28(3)	0.46(8)	9(2)
	-	0	0.81(9)	3.2(1)	37(4)

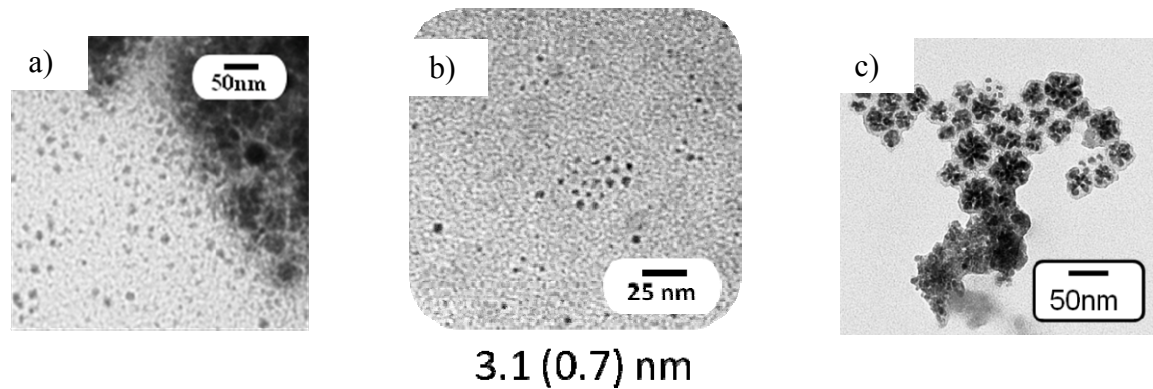


Figure 3S. TEM images of a) Re-dispersed NPs into BuMeIm [Tf₂N]; b) NPs obtained by sonochemical decomposition of Fe(CO)₅ into BuMeIm BF₄ (yield : 7 %); c) NPs obtained by sonochemical decomposition of Fe(CO)₅ with higher concentration (0.5 M) into BuMeIm [Tf₂N].

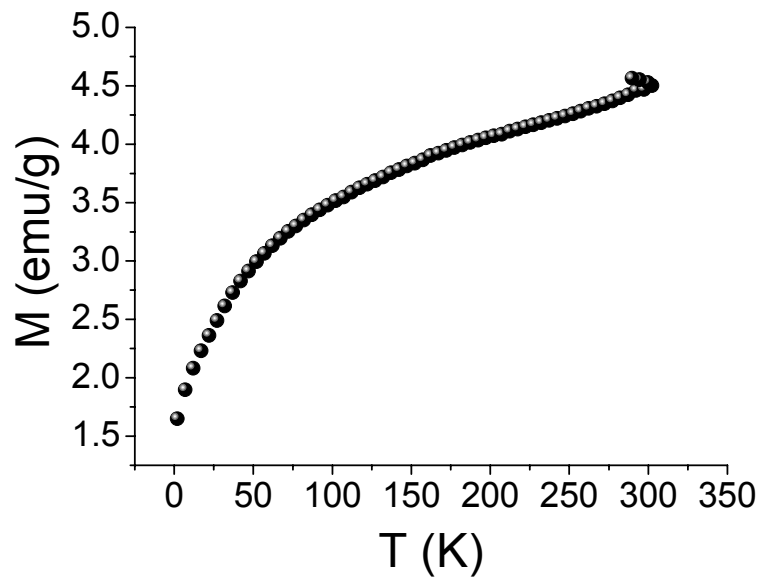


Figure 4S. Field Cooled (FC) (grey)/ Zero Field Cooled (ZFC) (black) magnetization curves performed under an applied magnetic field of 500 Oe.

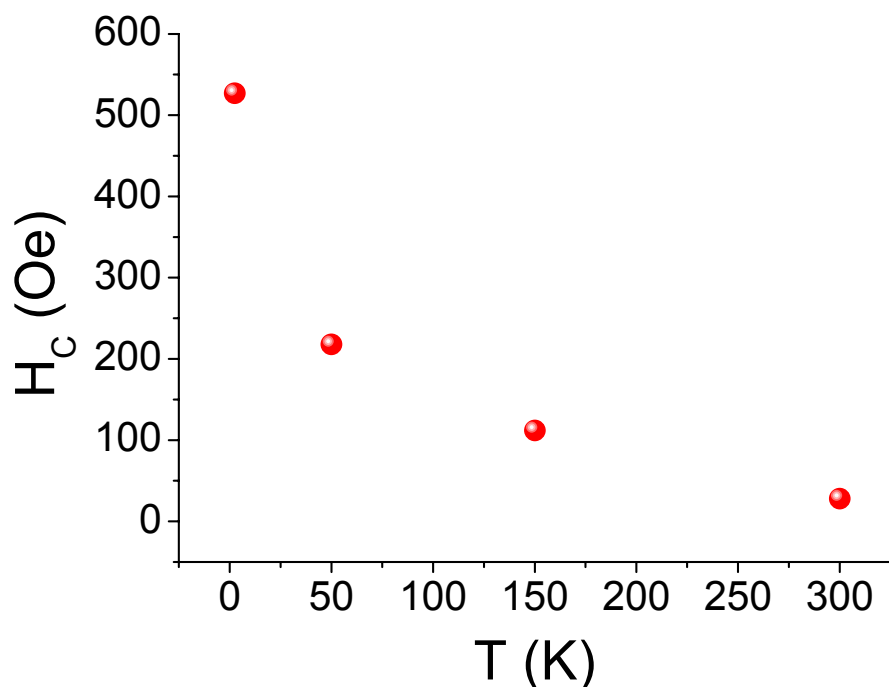


Figure 5S. Temperature dependence of the coercive field performed for iron NPs.

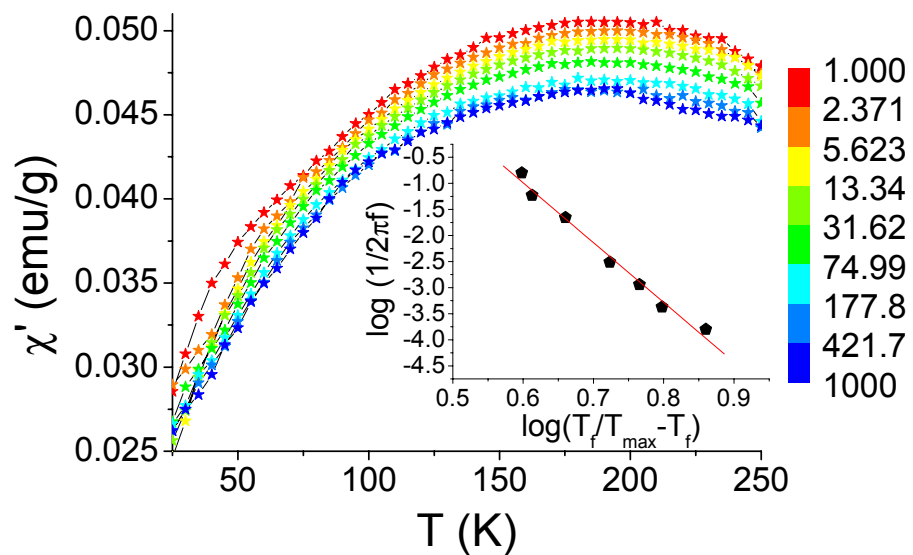


Figure 6S. AC susceptibility of iron nanoparticles performed with 8 frequencies in the 1 - 1000 Hz range logarithmic spaced. Insert : linear plot of the maximum temperature of each frequencies according to the critical scaling law.

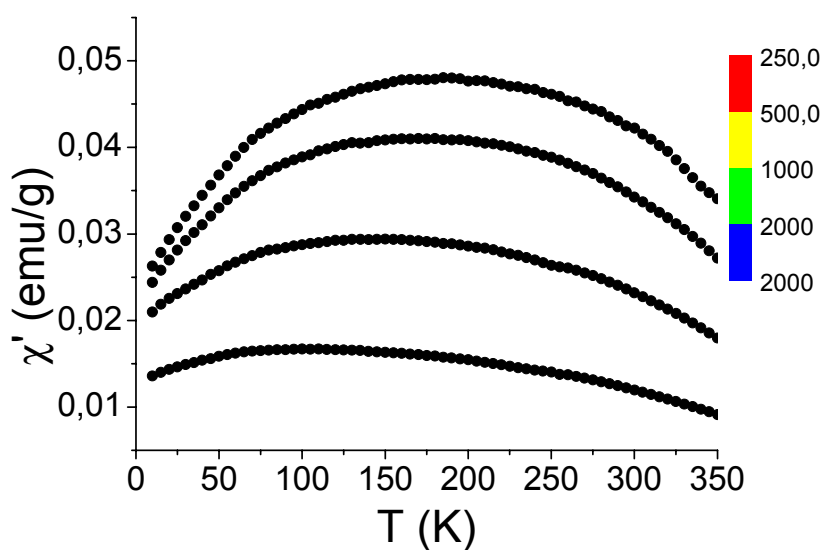


Figure 7S. Temperature dependence of the χ' component of ac susceptibility performed with different applied fields 250, 500, 1000, 2000 Oe for iron NPs

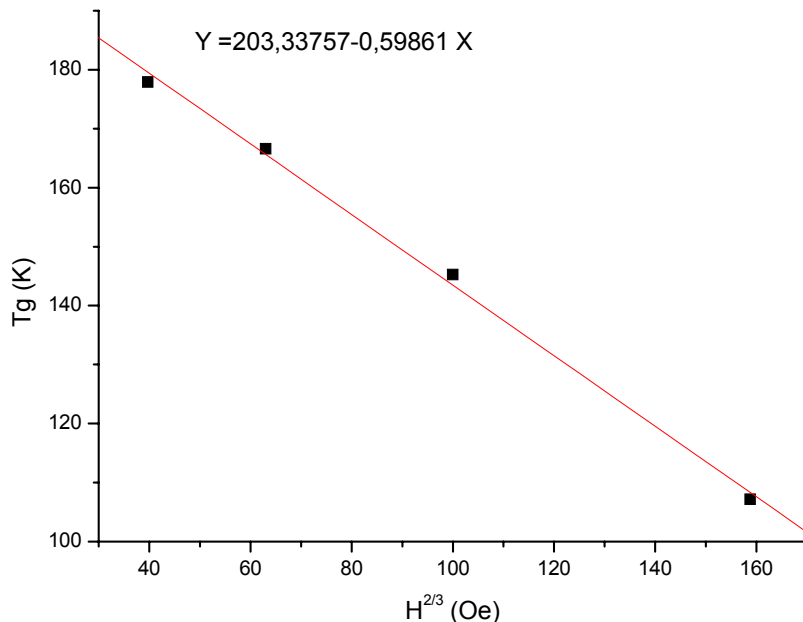


Figure 8S. Glassy temperature associated to the χ' peak position measured for 125 Hz plotted against $H^{2/3}$. The solid lines show a linear de Almeida – Thouless fit $H \propto [1 - (T_{\max} / T_g)]^{3/2}$ to the data. The obtained $T_g = 203$ K is close to T_{\max} obtained from the ZFC curve (184 K).

Thermal dependence of the relaxation time was fitted with the Arrhenius law, $\tau = \tau_0 \exp(E_a/k_B T)$, (E_a is the average energy barrier for the reversal of the magnetization, τ_0 is the attempt time and k_B is the Boltzmann constant) that gave unsatisfactory parameters: $\tau_0 = 1,78 \times 10^{-29}$ s and $E_a = 13251$ K and with the Vogel-Fulcher law, $\tau = \tau_0 \exp(E_a/k_B(T - T_0))$ (where an additional parameter T_0 takes into account interparticles magnetic interactions), giving the satisfactory parameter: $\tau_0 = 5.36 \times 10^{-11}$ s, $E_a = 2173$ K and $T_0 = 110$ K.